RGNZ/MGPB

Identification of Anthropogenic Materials in Lake Ciburuy Sediments Using Physico-Chemical Properties and Pollution Index

Rudarsko-geološko-naftni zbornik
(The Mining-Geology-Petroleum Engineering Bulletin)
UDC: 552.5
DOI: 10.17794/rgn.2023.4.10

Original scientific paper

Mileani Shafaria[1]; Kartika Hajar Kirana[2]; Dini Fitriani[3]; Eleonora Agustine[4]; Asep Harja[5]; Cipta Endyana[6]

[1]Program Study of Magister Physics, Faculty of Mathematics and Natural Sciences, Universitas Padjadjaran, Jl. Raya Bandung-Sumedang Km. 21, Jatinangor 45363, Indonesia, ORCID https://orcid.org/0009-0001-3473-7970

[2]Department of Geophysics, Faculty of Mathematics and Natural Sciences, Universitas Padjadjaran, Jl. Raya Bandung-Sumedang Km. 21, Jatinangor 45363, Indonesia, ORCID https://orcid.org/0000-0002-2772-3706

[3]Department of Geophysics, Faculty of Mathematics and Natural Sciences, Universitas Padjadjaran, Jl. Raya Bandung-Sumedang Km. 21, Jatinangor 45363, Indonesia, ORCID https://orcid.org/0000-0003-2143-9533

[4]Department of Geophysics, Faculty of Mathematics and Natural Sciences, Universitas Padjadjaran, Jl. Raya Bandung-Sumedang Km. 21, Jatinangor 45363, Indonesia, ORCID https://orcid.org/0000-0002-8020-653X

[5]Department of Geophysics, Faculty of Mathematics and Natural Sciences, Universitas Padjadjaran, Jl. Raya Bandung-Sumedang Km. 21, Jatinangor 45363, Indonesia, ORCID https://orcid.org/0000-0002-3534-4458

[6]Program Study of Geological Engineering, Faculty of Geological Engineering, Universitas Padjadjaran, Jl. Raya Bandung-Sumedang Km. 21, Jatinangor 45363, Indonesia, ORCID https://orcid.org/0000-0001-9448-1789

Abstract

Lake Ciburuy area is highly impacted by a wide range of human activities, including residential areas, rice fields, animal husbandry, plantations, dense vehicular traffic, and various industries, leading to the accumulation of pollutants. Particulates generated by the anthropogenic activities will be carried away and settle with the eroded soil to become sediment in the lake. This could cause serious problems in the aquatic environment if there is no monitoring study. Therefore, this study aimed to identify the anthropogenic material produced by human activities using physical and chemical properties analyses and pollution index calculations. The analysis of physical properties showed that Electrical Conductivity (EC), Total Dissolved Solid (TDS), and magnetic susceptibility were within the range of 30 – 790 µS/cm, 29 – 555 mg/L, 7.310 – 3431.956 $\times 10^{-8}$ m^3/kg, respectively. The X-ray diffraction (XRD) and the hysteresis parameter indicated that the samples contain ferrimagnetic materials, particularly magnetite with a mixture of Pseudo-Single Domain (PSD) and Multi-Domain (MD). The Scanning Electron Microscope (SEM) and Energy Dispersive Spectroscopy (EDS) identified the morphology of the magnetic mineral with different shapes, such as octahedral and spherule. Furthermore, the spherule shape indicated the presence of anthropogenic materials in the sample. In terms of chemical properties, this study measured the pH and Potential Toxic Elements (PTEs) in the sediments. The pH ranged from 7.2-8.9, while the PTEs showed moderate to very severe levels of contamination by Mn, Pb, Zn, Cd, and Cu, which exceeded the sediment quality standard. The PCA reveals the interconnection between physical and chemical properties, which can identify pollutants derived from anthropogenic materials, as well as indicate low, medium, and high levels of pollution in the lake area.

Keywords:
anthropogenic; physical and chemical properties; pollution index

1. Introduction

Lake Ciburuy is situated in Pamalayan Village, Bayongbong District, Padalarang, West Bandung Regency. Despite its proximity to bustling roads, residential areas, rice fields, and Citatah limestone mountain, it remains a vital ecosystem. Furthermore, the surrounding limestone area is used by private industries for cement and marble extraction. A large amount of human activity from residential areas, roads, rice fields, and industry can lead to the accumulation of anthropogenic material, leading to sedimentation in Lake Ciburuy.

The presence of anthropogenic materials in sediments can be identified by assessing the physical and chemical properties, such as the measurements of Electrical Conductivity (EC), Total Dissolved Solid (TDS), and magnetic parameters. Several studies used EC and TDS to determine sediment quality, including in the Ghorveh District, Iran (**Ayoubi et al., 2018**) and Lake Nkozoa, Cameroon (**Désirée et al., 2021**).

The analysis of magnetic parameters, including susceptibility, hysteresis, mineralogy, and morphology is often carried out using rock magnetic methods. These

Corresponding author: Kartika Hajar Kirana
e-mail address: kartika@geophys.unpad.ac.id

methods have been extensively used in studies investigating pollution derived from anthropogenic materials in sediment. Furthermore, they are considered to be rapid and environmentally friendly, making them a preferred non-destructive technique (**Evans and Heller, 2003**). The principle of these methods is that the magnetic properties of samples are caused by the characteristics of the constituent mineral grains, such as abundance, shape, and size (**Dearing, 1999**). The abundance of magnetic minerals in sediment is usually used as a proxy indicator of the presence of anthropogenic materials. This approach has been used in various studies carried out in Lake Wuhan, China (Yang **et al., 2009**), Citarum River (**Sudarningsih et al., 2017**), and Brantas River, Indonesia (**Mariyanto et al., 2019**). Several studies also utilized X-Ray Diffractometry (XRD) and hysteresis curves to identify the mineralogy and magnetic domain of sediment samples (**Tamuntuan et al., 2015**; **Yunginger et al., 2018**; **Kirana et al., 2021**). The morphology of magnetic minerals is often identified using SEM–EDS measurements. The SEM images of the sample affected by anthropogenic materials typically exhibit a unique feature, namely a spherule shape. Such images have also been observed in sediments from Lake South Sulawesi, Lake Maar (**Tamuntuan et al., 2010**), Meža River, Slovenia (**Miller and Gosar, 2015**), and Cikijing River (**Fitriani et al., 2021**).

The assessment of magnetic minerals is closely related to the abundance of Potential Toxic Elements (PTEs). Several studies highlighted the correlation between magnetic parameters and PTEs, thereby aiding the identification of anthropogenic material. This correlation has also been found in various locations, including in urban areas in Manchester, United Kingdom (**Robertson et al., 2003**), Lake Anonima, Antarctica (**Chaparro et al., 2017**), and Citarum River, Indonesia (**Sudarningsih et al., 2017**). Furthermore, the calculation of the pollution index can be used to determine the pollution level in a sediment sample based on the abundance of PTEs, which serve as indicators of contamination. Indices, such as I_{geo}, EF, CF, and PLI have been employed in studies in Lake Nasser, Africa (**Goher et al., 2014**), and Ganga River, India (**Pandey et al., 2015**). These areas were categorized as moderate, severe, and highly polluted regions based on PTEs concentrations, namely Cd and Pb derived from anthropogenic materials, such as industrial, agricultural, and mining.

Quantitative relationships have been reported among the physical-chemical properties of sediments. The association between several parameters of these properties has been extensively utilized in previous studies (**Schmidt, 2005**; **Spiteri et al., 2005**; **Yunginger et al 2018**; **Hamdan et al., 2022**). Multivariate analyses, such as Principal Component Analysis (PCA) and cluster analysis (CA) can be used to differentiate the influence of physical-chemical characteristics in sampling points. Furthermore, several studies reported the use of statistical methods in identifying environmental conditions in lakes (**Chapparo et al., 2017**; **Iswanto et al., 2020**; **Redwan et al., 2022**), rivers (**Pandey et al., 2015**), and city street dust (**Zhang et al., 2012**).

Over the past few decades, extensive studies focused on environmental evaluation using physical and chemical properties, specifically by examining the abundance of magnetic minerals and their relation to chemical characteristics. However, a study of physico-chemical parameters taking into account the abundance of magnetic minerals in sediments affected by volcanic rock and marble waste, such Lake Ciburuy has never been done before. Previous studies in Lake Ciburuy reported a positive correlation between the dissolved iron content and the abundance of Phytoconis sp (**Supriyatna et al., 2013**). A previous report also explored the preservation of Ciburuy Lake tourism area using the space utilization analysis method (**Nurqolbi et al., 2019**). Therefore, this study aims to examine the physical-chemical properties and their correlation to identifying pollutants derived from anthropogenic materials in volcanic area with influence of marble waste from limestone area. Although the method used to identify anthropogenic derived from pollution is commonly used by analyzing its physico-chemical properties, the use of pollution index calculations and multivariate analysis in the artificial reservoar influence by volcanic bedrock and carbonate from the marble industry has not been explored in the research area. The research will contribute as a reference for the physico-chemical properties of sediments in areas with similar geological characteristics.

2. Study Area

Lake Ciburuy is located in Pamalayan Village, Bayongbong District, Padalarang, West Bandung Regency, with coordinates of 107° 39’ 30” LS and 7° 12’ 30” BT. The geological condition of the study area is in the area of Qob rocks are the result of old volcanoes that are of Pleistocene age, including quaternary volcanic formations consisting of brexit, lava, and tuff with a deposition environment on land with a depth of 0 – 150 meters in the Cianjur Sheet Geological Map (**Sudjatmiko, 1972**). The topographical conditions at the sample points taken at Lake Ciburuy range from 700 – 710 meters above sea level (**Google Earth, 2022**). The Lake Ciburuy water system has an inlet and outlet. There are two inlet lines (water entering the lake): small rivers near residential areas that flow into the lake carrying domestic waste. Then the two outlet lines (water coming out of the lake) are irrigation lines for irrigating the rice fields and plantations of residents.

The environmental condition of Lake Ciburuy is close to the dense activities of roads, and the Citatah limestone mountain area, which private companies use to carry out

Copyright held(s) by author(s), publishing rights belongs to publisher, pp. 117-134, DOI: 10.17794/rgn.2023.4.10

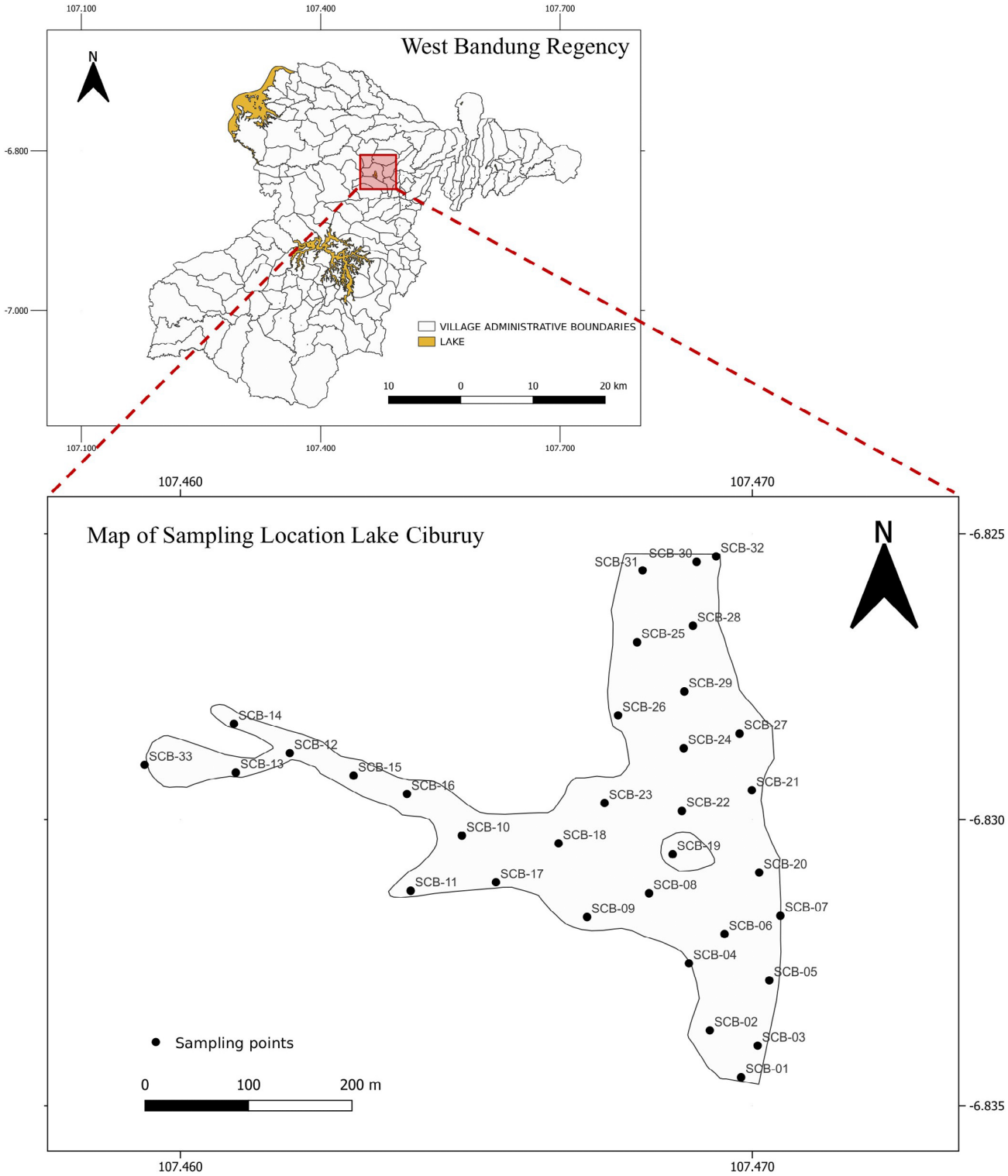

Figure 1: Map of Lake Ciburuy. The red box shading shows the location of sampling points in Lake Ciburuy

lime mining and establish industrial areas such as cement and marble factories. Moreover, Lake Ciburuy is surrounded by residential and home industry areas. Waste from residential areas and industrial areas is indicated to enter the lake body and then deposited along with sediments derived from its bottom rock and can pollute the lake.

3. Material and Methods

All samples taken from Lake Ciburuy are surface sediments. Surface sediment samples refer to sediments at a depth of 0-15 cm at the sediment-water interface. The sediment cores were not used in this research. Sediment samples were taken using a Ponar grab sampler

Copyright held(s) by author(s), publishing rights belongs to publisher, pp. 117-134, DOI: 10.17794/rgn.2023.4.10

from 33 sampling points scattered in the edge, middle, outlet, and marble industry waste dump at Lake Ciburuy, as shown in **Figure 1**. The sampling points from the inlet are SCB–04, SCB–30, and SCB–32, while the sampling points from the outlet are SCB–02 and SCB–28. The sampling points of SCB-33 are located near the marble industry waste dump, which is characterized by predominantly white-coloured sediments. The samples obtained from the region were then prepared for drying and sieving processes. Sieving was carried out with a mesh size of 10 to remove impurities, such as plant roots and plastic waste while allowing sand grains with an approximate size of 2,000 mm to pass through.

3.1 Physical Properties

The measurements of EC, TDS, and pH of the samples were conducted using the Hanna Combo Meter type HI-9813-6 pH/EC/TDS/°C Portable Meter. The EC and TDS measurements conducted to identify the amount of material dissolved in water and its ability to conduct the electric current, while pH measurements were carried out to determine the degree of acidity. The higher value of EC, the higher value of TDS, which means that the more dissolved substances and the more polluted. Furthermore, the samples were prepared for magnetic susceptibility measurements to measure the abundance of magnetic minerals (**Yang et al., 2009**; **Mariyanto et al., 2019**; **Kirana et al., 2021**). The sediments obtained were placed into a 10 cm^3 volume holder for magnetic susceptibility measurement using the Bartington MS2B Magnetic Susceptibility meter. This instrument measured volume-based-magnetic susceptibility with dual frequency, namely κ_{LF} for low frequency-magnetic susceptibility at 460 Hz and κ_{HF} for high frequency-magnetic susceptibility at 4600 Hz. The measured parameter was then calculated to determine the mass-based-magnetic susceptibility value, with χ_{LF} and χ_{HF} for low and high frequencies, respectively. Apart from determining the magnetic mineral, the parameter could also be used to identify the superparamagnetic grain in the sample through the calculation of frequency-dependent magnetic susceptibility ($\chi_{FD}\% = [(\chi_{LF} - \chi_{HF})/ \chi_{LF}] \times 100\%$).

The XRD was measured using the Rigaku X-Ray Diffractometer. This measurement uses a small amount of powder sample that produce by the preparation process. The bulk sediment was disaggregated in a 100 ml beaker glass and distilled water to avoid lumps on the sediment. Then, the samples are centrifuged to remove some organic residue (**Cook et al., 1975**). The XRD measurement helped to identify the dominant mineral contained in the samples. Furthermore, the hysteresis parameters were measured using the Oxford type 1.2H Vibrating Sample Magnetometer. This measurement produced the plot between the magnetization M (Am^2kg^{-1}) and the applied field H (T). The plot provided information on some hysteresis parameters including saturation remanent magnetization (M_{rs}), saturation magnetization (M_s), remanent coercivity (H_{cr}), and coercivity field (H_c). The hysteresis curve could be used to determine the magnetic domain by replotting the hysteresis parameters. This involved creating a plot that related the ratio of magnetization at remanent saturation to the magnetization at saturation (M_{rs}/M_s) with the ratio of the field at remanent coercivity and the field at coercivity (H_{cr}/H_c), commonly known as Day's plot. The scanning electron microscope-energy dispersion spectroscopy (SEM-EDS) was performed using the JEOL JSM-6510A. The sample conducted the extraction process before measurement by magnetic stirrer to identify the morphology of magnetic minerals.

3.2 Chemical Properties

Inductively Coupled Plasma-Optical Emission Spectrometry (ICP-OES) measurements were performed to determine the abundance of elements content using the Inductively Coupled Plasma Agilent 725 Series ICP-OES. The preparation sample process for measuring ICP analysis uses leaching and wet destructive methods with $HNO_3 + HClO_4$. The measured elements consisted of As, Cd, Co, Cr, Cu, Fe, Mn, Ni, Pb, and Zn. The results were then compared with the sediment quality standards around the world through Sediment Quality Guidelines (SQGs). Subsequently, the value of each element content was used to calculate the pollution index, which consisted of the Index of Geoaccumulatuion, Enrichment Factor (EF), Contaminant Factor (CF), and Pollution Load Index (PLI).

3.2.1 Index Geo-accumulation (I_{geo})

The calculation of the Index of Geoaccumulation (I_{geo}), as calculated in Equation 1, was used to measure the enrichment of elements by comparing their abundance with the background value. Furthermore, the index was calculated using the method proposed by **Muller (1969)**. In Equation 1, C_n represented the concentration value of the element in the sample, while B_n was the concentration of background value in the soil (see world shale elements concentration in **Wedepohl, 1971**). The calculated value of I_{geo} was then divided into several classes, with a range of I_{geo} values ≤ 0, unpolluted; $I_{geo} \leq 1$, unpolluted to moderately polluted; $I_{geo} \leq 2$, moderately polluted; $I_{geo} \leq 3$, moderately to highly polluted; $I_{geo} \leq 4$, highly polluted; $I_{geo} \leq 5$, highly to very highly polluted; and $I_{geo} > 5$, very highly polluted.

$$I_{geo} = \log_2 (C_n / 1.5B_n) \quad (1)$$

3.2.2 Enrichment Factor (EF)

The calculation of EF was used to evaluate the magnitude of contamination in the environment. EF was calculated by considering the abundance of PTEs in sediments with reference to both element concentrations and background values obtained from the Earth's core

Copyright held(s) by author(s), publishing rights belongs to publisher, pp. 117-134, DOI: 10.17794/rgn.2023.4.10

(**Wedepohl, 1971**). Furthermore, the commonly used reference metals included Fe, Mn, and Al (**Barbieri et al., 2016**). EF was calculated using Equation 2, where C was the concentration of elements in the sample, C_r was the concentration of the reference element (in this case using Fe element), B was the background value of an element, and B_r was the background value of the reference element (Fe). Fe is a major component of the Earth's crust and stable element (**Abderrahmane et al., 2021**). The EF value was classified into different classes: EF <1, no enrichment; EF 1–3, minor enrichment; EF 3–5, moderate enrichment; EF 5–10, moderately severe enrichment; EF 10–25, severe enrichment; EF 25–50, very severe enrichment; and EF >50, extremely severe enrichment (**Hakanson et al., 1980**).

$$EF = (C/C_r)/(B/B_r) \quad (2)$$

3.2.3 Contaminant Factor (CF) and Pollution Load Index (PLI)

CF was calculated to estimate the level of contamination in the sediment studied compared to the background value, as presented in Equation 3. PLI assessed the total pollution levels and sediment toxicity in the study area (**Tomlinson et al., 1980**), and its calculation is presented in Equation 4.

$$CF = C_m/B_m \quad (3)$$

$$PLI = (CF1 \times CF2 \times CF3\ldots \times CFn)^{1/n} \quad (4)$$

C_m is the measured concentration of elements and B_m is the background value of the same type of elements. The value of CF was classified into CF < 1 = low; CF 1–3 = moderate; CF 3–6 = considerable; and CF > 6 = very high contaminant. In Equation 4, CF_n is the contamination of each element and the PLI value was classified into two categories, namely PLI < 1 = unpolluted and PLI > 1 = polluted (**Tomlinson et al., 1980**).

3.3 Statistical Analysis

Statistical analysis was carried out on the data of the physical and chemical properties of sediments from Lake Ciburuy using 11 samples related to the number of samples measured on PTEs. Furthermore, bivariate analysis of variables was calculated using Pearson's product-moment correlation. The principal component analysis (PCA) was performed to identify the cluster of correlations between the parameters. The statistical analysis was carried out using R, an open-source software (version 4.2.1 2022).

Table 1: The value of pH, EC, TDS, χ_{LF}, χ_{HF}, and χ_{FD}% in all samples.

Sample ID	EC (µS /cm)	TDS (mg/l)	pH	χ_{LF} ($\times 10^{-8}$ m^3/kg)	χ_{HF} ($\times 10^{-8}$ m^3/kg)	χ_{FD}%
SCB–01	220	167	7.0	915.28	887.15	3.07
SCB–02	210	157	7.6	1001.98	963.55	3.84
SCB–03	280	210	7.6	878.69	850.86	3.17
SCB–04	230	174	7.5	717.02	680.79	5.05
SCB–05	450	311	7.4	3431.96	3387.43	1.30
SCB–06	500	367	7.4	470.15	442.78	5.82
SCB–07	420	305	7.4	987.76	954.60	3.36
SCB–08	460	349	7.4	413.14	388.54	5.96
SCB–09	560	400	7.5	433.65	410.98	5.23
SCB–10	360	258	7.7	806.93	786.29	2.56
SCB–11	120	111	8.0	876.91	866.08	1.24
SCB–12	230	177	7.8	1143.66	1128.93	1.29
SCB–13	160	117	7.9	724.66	712.60	1.66
SCB–14	180	144	7.7	2211.57	2188.16	1.06
SCB–15	280	202	7.6	1038.58	1014.96	2.27
SCB–16	240	179	7.8	2126.86	2095.13	1.49
SCB–17	430	309	7.7	581.09	563.16	3.08
SCB–18	250	192	7.6	663.12	636.13	4.07
SCB–19	270	212	7.5	1541.69	1508.49	2.15
SCB–20	360	263	7.5	1493.94	1450.41	2.91
SCB–21	410	312	7.5	781.72	747.48	4.38
SCB–22	320	240	7.4	2303.10	2241.32	2.68
SCB–23	430	340	7.5	658.53	625.07	5.08
SCB–24	790	555	7.4	399.80	372.35	6.87
SCB–25	530	432	7.4	713.15	676.14	5.19
SCB–26	500	363	7.3	663.88	628.94	5.26
SCB–27	520	390	7.5	597.79	566.07	5.31
SCB–28	540	413	7.5	578.43	545.54	5.69
SCB–29	750	548	7.4	511.13	477.88	6.51
SCB–30	540	394	7.5	1054.58	1021.90	3.10
SCB–31	660	487	7.2	582.64	550.24	5.56
SCB–32	530	409	7.2	1045.56	1012.33	3.18
SCB–33	30	29	8.9	7.31	7.07	3.29
Max	790.00	555.00	8.9	3431.96	3387.43	6.87
Min	30.00	29.00	7.0	7.31	7.07	1.06
Mean	386.67	288.36	7.6	980.49	951.19	3.72
Median	410.00	305.00	7.5	781.72	747.48	3.29
Standard Deviation	179.29	129.12	0.3	680.66	675.22	1.69

4. Result

Table 1 shows the results of sediment sample measurements, where a pH range of 7.2 – 8.9 was obtained with an average of 7.6 ± 0.3. The value of EC ranged from 30 – 790 µS/cm with an average of 386.67 ± 179.29 µS/cm. Furthermore, the TDS of the sediment samples ranged from 29 – 555 mg/L with an average of 288.36 ± 129.12 mg/L. The highest value of EC and TDS was obtained in SCB–24 located in the middle of Lake Ciburuy,

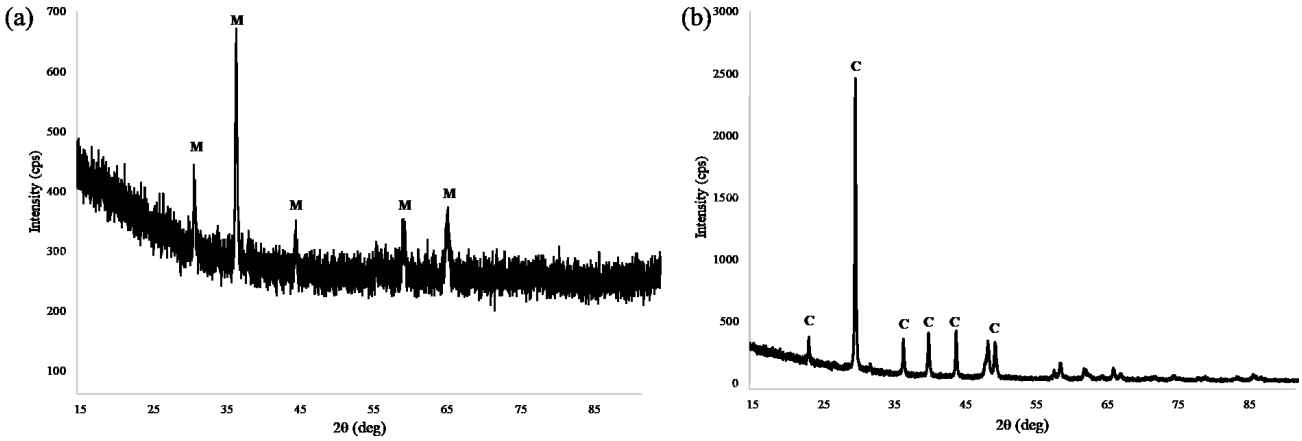

Figure 2: XRD Diffractogram for two representative sediment samples (a) SCB–05: diffractogram peaks dominated by magnetite (Fe_3O_4) mineral (M); (b) SCB–33: diffractogram peaks dominated by calcite ($CaCO_3$) mineral (C).

Table 2: The abundance of potential toxic elements (PTEs) of sediment samples (N = 11). n.d: not detected, SD: Standard Deviation, TEL: threshold effect level.

Sampel ID	Fe (mg/kg)	Mn (mg/kg)	Ni (mg/kg)	Pb (mg/kg)	Zn (mg/kg)	As (mg/kg)	Cd (mg/kg)	Co (mg/kg)	Cr (mg/kg)	Cu (mg/kg)
SCB–01	**22205.80**	**8549.10**	**56.49**	**182.10**	**689.84**	13.12	**10.39**	47.38	57.89	**558.71**
SCB–05	**23246.75**	**13325.75**	16.06	**166.58**	**535.81**	11.77	**10.46**	50.89	**81.95**	**429.41**
SCB–06	18480.31	**12785.38**	0.99	**178.34**	**575.26**	7.73	**9.04**	30.28	50.20	**433.50**
SCB–09	17512.26	**12347.41**	**67.29**	**179.37**	**1182.16**	11.30	**10.03**	29.36	66.48	610.78
SCB–10	17419.56	**14036.09**	**37.99**	**131.77**	**910.64**	4.05	**7.05**	40.96	62.73	**367.10**
SCB–12	9727.37	**3420.14**	**30.62**	**108.24**	**497.13**	8.05	**4.86**	21.82	52.29	**259.62**
SCB–13	7728.47	**4138.78**	18.59	**57.21**	**400.10**	16.57	**4.39**	12.97	32.52	**140.96**
SCB–19	**25618.92**	**27414.80**	n.d	**135.11**	**312.01**	**22.28**	**11.42**	44.98	**91.83**	**447.29**
SCB–29	**21665.28**	**17048.81**	n.d	**172.85**	**491.46**	5.75	**10.74**	47.23	47.11	**451.72**
SCB–30	**23134.32**	**11300.05**	n.d	**206.04**	**654.80**	9.34	**10.86**	69.89	60.22	**517.10**
SCB–33	816.50	**1007.68**	n.d	7.86	8.20	**25.04**	**3.12**	5.02	14.86	54.68
Max	25618.92	27414.80	67.29	206.04	1182.16	25.04	11.42	69.89	91.83	610.78
Min	816.50	1007.68	0.99	7.86	8.20	4.05	3.12	5.02	14.86	54.68
Mean	17050.50	11397.64	32.57	138.68	568.85	12.27	8.40	36.43	56.19	388.26
Median	18480.31	12347.41	30.62	166.58	535.81	11.30	10.03	40.96	57.89	433.50
SD	7766.35	7310.26	23.37	60.28	305.95	6.64	3.00	18.70	21.22	172.00
Threshold Value (mg/kg)	20000[(b)]	248.77[(c)]	21[(a)]	50[(a)]	200[(a)]	20[(a)]	1.5[(a)]	-	80[(a)]	65[(a)]
TEL	-	-	18[(d)]	35[(d)]	123[(d)]	5.9[(d)]	0.6[(d)]	-	37.3[(d)]	35.7[(d)]

[a]Australian and New Zealand Environment and Conservation Council Interim Sediment Quality Guideline (ANZECC ISQG-low, 2000)
[b]Guideline for The Protection and Management of Aquatic Sediment Quality in Ontario (1993),
[c]National Sediment Quality Survey US EPA (2004).
[d]Burton (2002)

while the lowest was recorded in SCB–33 located in the marble waste dump. The results of low-frequency magnetic susceptibility (χ_{LF}) value showed a range of 7.31 – 3431.96 × 10^{-8} m^3/kg with an average of 1010.905 × 10^{-8} m^3/kg. The value of high-frequency magnetic susceptibility (χ_{HF}) in the study area ranged from 7.07 – 3387.43 × 10^{-8} m^3/kg, with an average of 980.696 × 10^{-8} m^3/kg. The highest value of magnetic susceptibility was found in SCB–05 at the edge of the lake where a lot of waste was piled up. The frequency-dependent magnetic susceptibility (χ_{FD}%) showed a range of 1.06% – 6.88% with an average of 3.717%.

Figure 2 shows the results of the measurement of XRD on SCB–05 and SCB–33. The peak of the diffrac-

Copyright held(s) by author(s), publishing rights belongs to publisher, pp. 117-134, DOI: 10.17794/rgn.2023.4.10

togram of each sample showed that SCB–05 was dominated by magnetite minerals (Fe_3O_4), while calcium carbonate/calcite minerals ($CaCO_3$) were dominant in SCB–33. Furthermore, **Figure 3** shows the shape of a hysteresis curve with a relatively narrow gap indicating a minor contribution of paramagnetic minerals or a greater contribution of ferrimagnetic minerals (**Tamuntuan et al., 2015**). The ferrimagnetic mineral on this hysteresis curve was considered to contain magnetite because it saturated before 0.3 T (**Moskowitz, 1999**; **Gehring et al., 2009**). The saturation magnetization (M_s), remanence saturation magnetization (M_{rs}), coercivity magnetic field (H_c), the coercivity of remanence magnetic field (H_{cr}) for SCB–05 was 35.53 (emu/g), 9.57 (emu/g), 0.034 (T), and 0.035 (T), respectively, For SCB–24, the values obtained were 21.44 (emu/g), 7.43 (emu/g), 0.0 196 (T), and 0.035 (T), respectively. In SCB–32, the values were 28.47 (emu/g), 7.62 (emu/g), 0.0313 (T), and 0.035 (T), respectively. **Figure 4** shows the results of SEM-EDS measurement, where the SEM image of SCB–05 showed the morphological shape of magnetite minerals, namely octahedral and spherule. Meanwhile, the SEM image for SCB–33 showed the presence of irregular magnetic aggregates. The EDS analysis showed high concentrations of Fe and O, which were suspected to be carriers of the mineral magnetite (Fe_3O_4).

Table 2 shows the content of the elements in the sediment samples. The highest to the lowest means value of elements content was Fe (17050.50 mg/kg), Mn (11397.64 mg/kg), Zn (568.85 mg/kg), Cu (388.26 mg/kg), Pb (138.68 mg/kg), Cr (56.19 mg/kg), Co (36.4 mg/kg), Ni (32.57 mg/kg), As (12.27 mg/kg), and Cd (8.40 mg/kg).

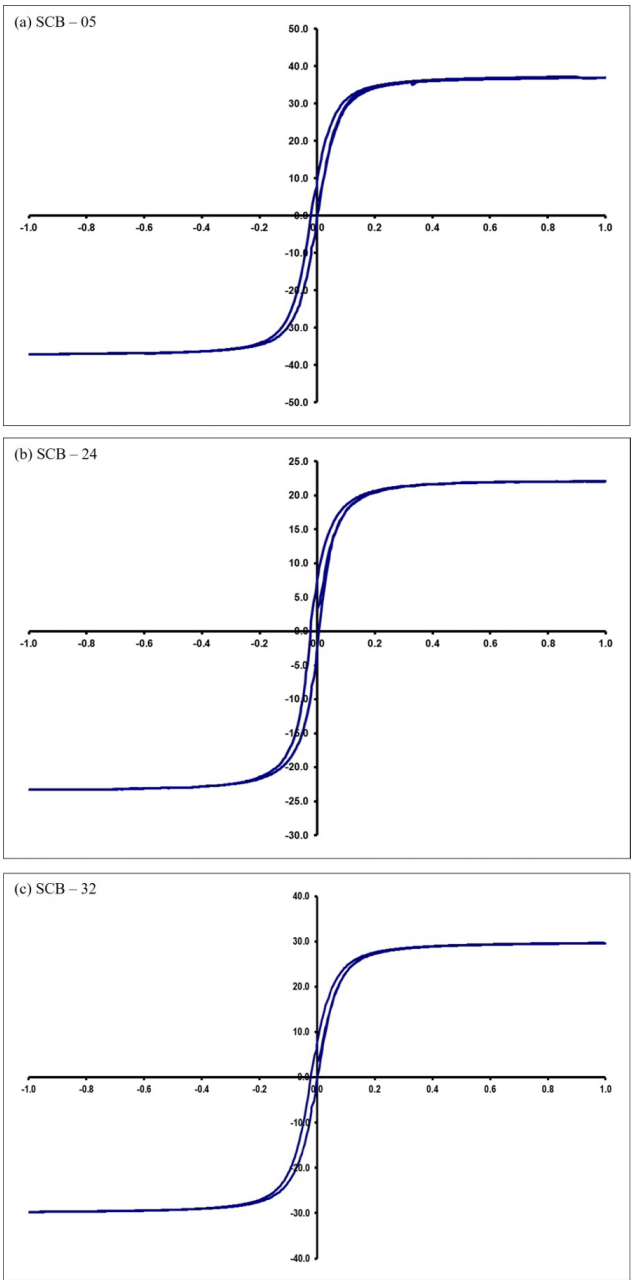

Figure 3: Hysteresis parameter of (a) SCB–05, (b) SCB–24, (c) SCB–32.

5. Discussion

5.1 Physical Properties

The EC value of the sample was influenced by several community activities, such as netting fish using pellets. The fish pellets had several compositions, including salt minerals, which could increase salinity and the ability of water to conduct electricity (**Herbatani, 2021**). Furthermore, a high value of EC could be caused by the presence of high levels of ionized dissolved salt in the sediment. The results showed that the TDS values were strongly influenced by weathering of rocks, runoff from the soil, and anthropogenic factors in the form of domestic and industrial waste. The highest TDS value was obtained at the SCB–24 and this was in line with the EC measurements, where the highest value was also recorded at the same point. Based on these findings, EC and TDS had a significant correlation and they could influence each other, as shown in **Table 3**. The results showed that the higher the EC value, the higher the TDS. This was because EC was a measure of the capacity of an object to conduct an electric charge. Its ability depended on the concentration of dissolved ions, ionic strength, and measurement temperature. The concentration of dissolved ions was often measured using TDS. Therefore, EC and TDS measurements with the same trend value indicated high accuracy in the results (**Rusydi, 2018**). Similar findings were also obtained in previous Indian studies, where a strong correlation was found between EC and TDS parameters with a directly proportional relationship (**Madhulekha and Agarwal, 2017**). **Table 3** strengthened this analysis by presenting the results of a highly significant correlation between the two parameters, with a correlation coefficient of 0.98 ($p < 0.01$).

The value of χ_{LF} and χ_{FD}% varied in this study due to the influence of different sediment sources at various sampling points. Based on the magnetic susceptibility

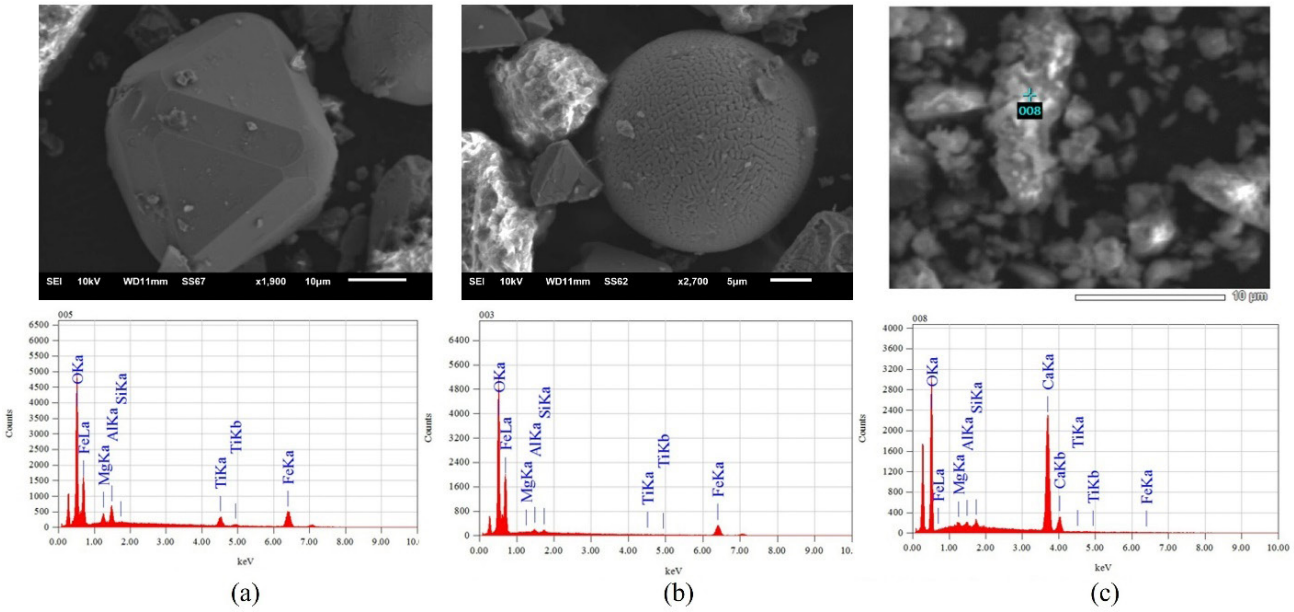

Figure 4: Results of SEM-EDS (a) SCB–05: showing of octahedral shaped-magnetic grains; (b) SCB–05: showing of spherule shaped-magnetic grains; (c) SCB–33: showing of irregular magnetic aggregates shaped grains.

value, Lake Ciburuy sediments were dominated by ferrimagnetic minerals except for SCB–33, which was influenced by paramagnetic components. Based on **Dearing (1999)**, ferrimagnetic minerals typically exhibited magnetic susceptibility values of > 10×10^{-8} m^3/kg. Meanwhile, if the susceptibility was below this threshold, then it was considered paramagnetic property.

Figure 5 shows the value of χ_{LF} and χ_{FD}% of sediment samples at each sampling point. In the sampling point of Lake Ciburuy, a high value of χ_{LF} was often accompanied by a low χ_{FD}%. For example, the highest value of χ_{FD}% in the north of the lake (SCB–24) showed a low χ_{LF}. Furthermore, the distribution χ_{LF} at the lakeside area showed lower values compared to those in the middle of the lake except SCB–05. **Ramasamy et al., (2022)** classified the magnetic susceptibility in beach and intertidal sediment into high (more than 100×10^{-8} m^3/kg) and very high (more than 500×10^{-8} m^3/kg) categories. Based on these findings, the sediments on Lake Ciburuy had a high and very high value of magnetic susceptibility. SCB-33 showed the smallest magnetic susceptibility because the samples were taken from marble waste dumps. The average value of χ_{FD}% from all samples was approximately 3.717%, indicating that the sample had a small superparamagnetic grain contribution (SP). Meanwhile, a χ_{FD}% value of 2%-10% indicated a mixture of superparamagnetic and non-superparamagnetic coarse grains (**Dearing, 1999**). Samples with values ranging from 1–4% showed the presence of anthropogenic material (**Bijaksana and Huliselan, 2010**). Based on the results, the sediment samples were affected by anthropogenic material, but some were influenced by pedogenic.

Geologically, Lake Ciburuy was formed from an old Pleistocene volcano and had the Quaternary volcanic formation, consisting of breccias, lava, lava, and tuff. Magnetic susceptibility measurements were carried out for volcanic bedrock in Brantas River, East Java, Indonesia, with a range of (844.0-7231.4) × $10^{-8}m^3/kg$ (**Mariyanto et al., 2019**). Brantas River flowed through Mounts Arjuno and Kelud, both of which had bedrock in the form of lava, volcanic breccia, tuff breccia, and tuff. Furthermore, the magnetic susceptibility of the surface sediment samples taken from Brantas River showed an approximate value of 3164.2 × $10^{-8}m^3/kg$. Apart from being influenced by the bedrock of the study area, the value obtained was influenced by the magnetic properties of a combination of lithogenic and anthropogenic materials (**Adeloka and Eletta, 2007**). The presence of anthropogenic material could also influence the high magnetic susceptibility in the sediments, such as industrial dust, dust containing magnetic particles, and magnetic particles originating from vehicle emissions accompanied by increased concentrations of PTEs (**Dankoub et al., 2012**). The value could also be decreased due to pedogenic processes and an increase in the abundance of diamagnetic materials, such as calcite (**Ayoubi et al., 2018**). Lake Ciburuy received an increase in calcite because there was a marble industry with a waste disposal site around the area. In **Table 1**, the highest magnetic susceptibility value in Lake Ciburuy was approximately 3431.96 ×$10^{-8}m^3/kg$. The results showed that Brantas River with the influence of volcanic bedrock also had a similar value ($3164.2\times10^{-8}m^3/kg$). Consequently, the sampling point with the highest value in Lake Ciburuy was influenced by bedrock and anthropogenic material sources. Based on these findings, the influx of anthropogenic material sources into the sediment could reduce magnetic susceptibility. This was because the study area had been affected by diamagnetic materials, such as calcite contained in marble sediment samples at SCB-33.

Copyright held(s) by author(s), publishing rights belongs to publisher, pp. 117-134, DOI: 10.17794/rgn.2023.4.10

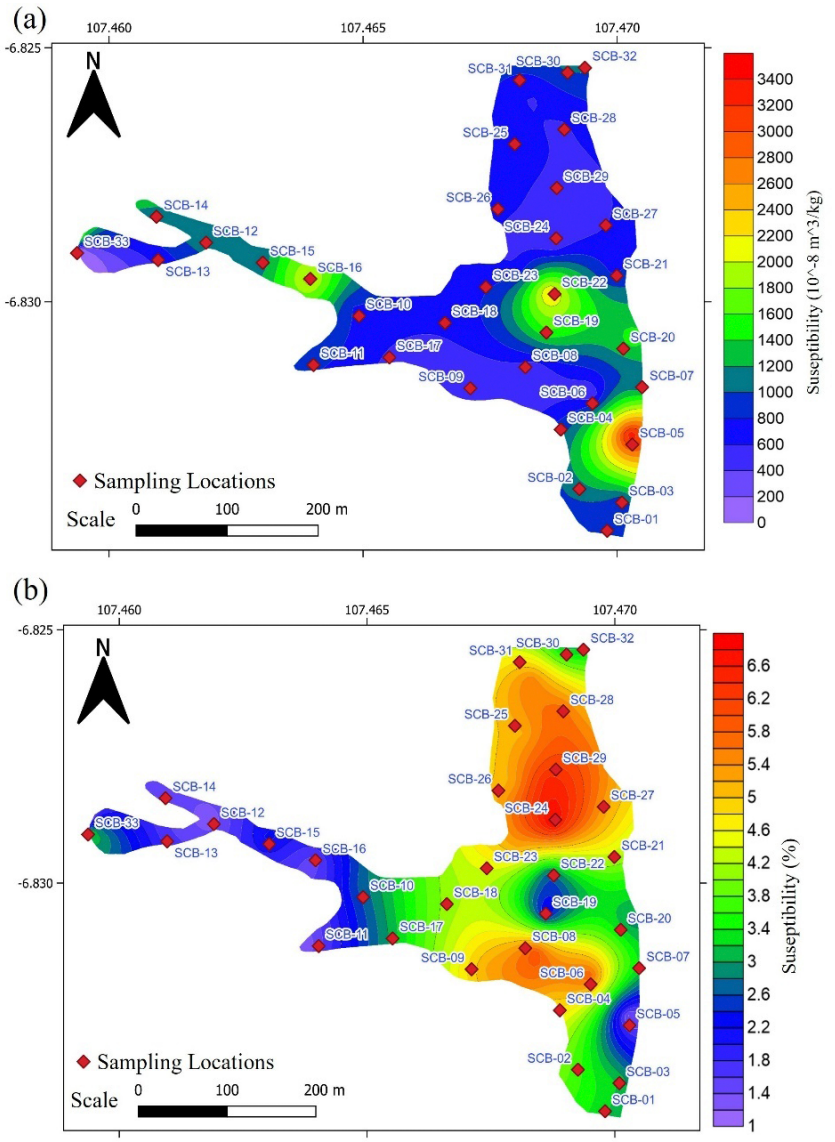

Figure 5: Map of the distribution of magnetic susceptibility values (a) distribution of low-susceptibility values (χ_{LF}), the color scale towards red indicates a higher χ_{LF} values and (b) distribution of dependent-susceptibility values (χ_{FD}%), the color scale towards red indicates a higher χ_{FD}% values.

Figure 6 shows a scattergram derived from the plot of χ_{LF} and χ_{FD}%, which was used to determine the distribution of the magnetic domains contained in the sample. The analysis showed the dominance of the magnetic domains in the Stable-Single Domain (SSD) or Multi-Domain (MD). Furthermore, the samples exhibited a mixture of sizes, including superparamagnetic (SP) grains and grains larger than >0.005 µm. **Solomon et al., (2017)** state that the MD and SP grains were derived from anthropogenic and natural sources (lithogenic). The results showed that the sediment samples contained anthropogenic materials was strengthened by the correlation between χ_{LF} and χ_{FD}%. **Table 3** shows a negative correlation between χ_{LF} and χ_{FD}% (r = 0.558; p<0.10), indicating that anthropogenic minerals contributed more to the abundance of magnetic minerals than their natural or pedogenic carrier variant (**Lu et al., 2007**).

The results of Day's plot of the SCB–05 and SCB–32 showed that the grain size was a mixture of single-domain (SD) and multi-domain (MD), as shown in **Figure**

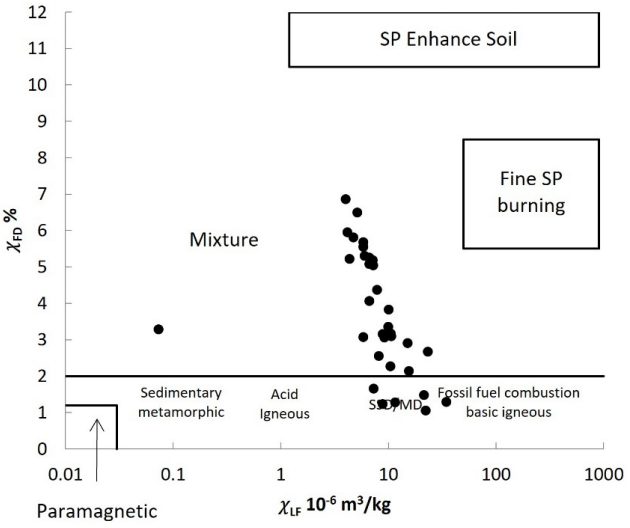

Figure 6: Scattergram plot of χ_{LF} and χ_{FD}% value showed by dot marks for all samples (N = 33) dominated by mixture and SSD/MD grains. SP: Superparamagnetic; SSD/MD: Stable-Single Domain/Multi-Domain.

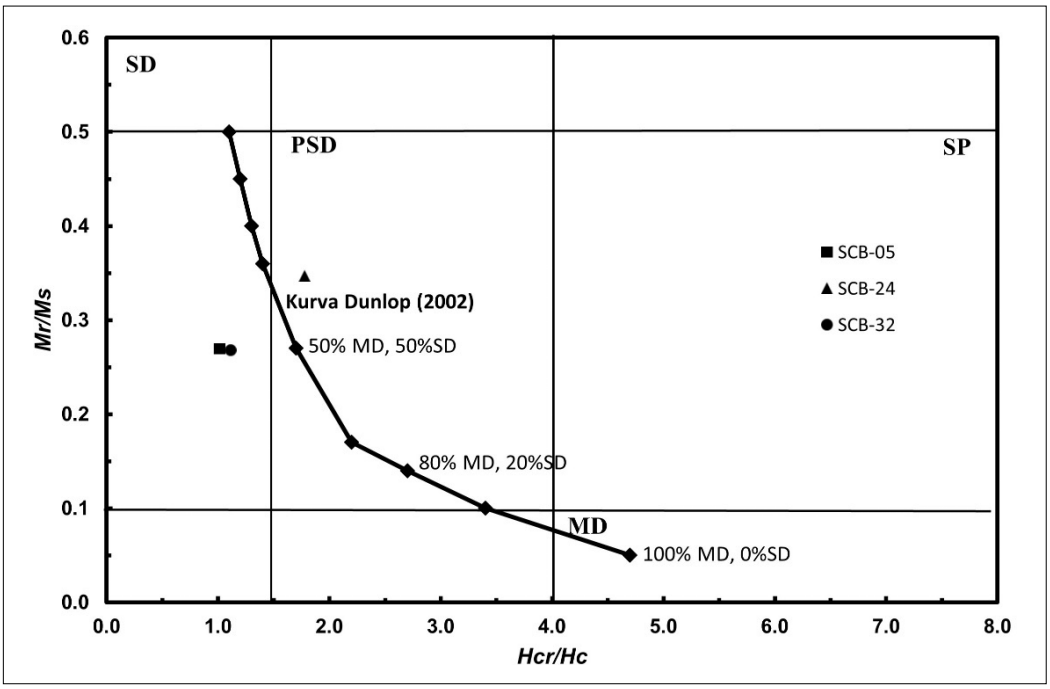

Figure 7: Day plot of SCB–05 (rectangle mark), SCB–24 (triangle mark), and SCB–33 (dot mark) are predominantly falls in the PSD zone. Black line and diamond marks represent percentage of SD-MD abundance in samples adopted from Dunlop (2002).
SD: Single-Domain; MD: Multi-Domain; PSD: Pseudo-Single Domain; SP: Superparamagnetic.

7. Meanwhile, the SCB–24 sample was in the pseudo-single domain (PSD) zone. Magnetic minerals dominated by PSD and a mixture of SD-MD grains were also found in the river and lake sediments in other locations (**Yang et al., 2009**; **Zhang et al., 2012**; **Su et al., 2013**; **Tamuntuan et al., 2015**; **Sudarningsih et al., 2017**; **Mariyanto et al., 2019**).

The different shapes of the morphology of magnetic grain could indicate that they were formed from different sources. The octahedral shape indicated the presence of a magnetic mineral, either from a pedogenic origin. **Figure 4a** shows an octahedral image representing natural grains of magnetite that could be obtained from weathering rocks and had a rough surface with damage at the corners (**Tamuntuan et al., 2010**). Meanwhile, the spherule form indicated a change in shape of magnetic minerals caused by oxidation or combustion and the process of diagenesis (**Franke et al., 2007**). The SEM results of SCB–33 showed the presence of irregular aggregate magnetic minerals. The EDS analysis in the SCB–33 showed a high content of Ca and O, which were suspected to be carriers of $CaCO_3$. The presence of Ca and O in the sample was similar to marble waste with the same components. The CaO material had diamagnetic properties (**Dearing, 1999**). This is indicating that marble waste mixing with volcanic soil could weaken the magnetic characteristics. Volcanic soils were known to have strong magnetic and ferrimagnetic properties. The mixture of these characteristics could lead to the formation of a paramagnetic.

5.2 Chemical Properties

Based on ICP-OES measurement (see **Table 2**), the abundance of PTEs could be used to determine sediment quality by comparing the reference sediment quality values around the world (SQGs). The results of PTEs showed that the abundance of sediments in Lake Ciburuy had exceeded the standard threshold in other countries (ANZECC ISQG-Low, US EPA, and Canadian SQGs). The only exception was the As element, which did not exceed the quality standard value in SCB–01, SCB–05, SCB–06, SCB–09, SCB–10, SCB–12, SCB–13, SCB–29, and SCB–30, as well as Cr element in SCB–01, SCB–06, SCB–09, SCB–10, SCB–12, SCB–13, SCB–29, and SCB–30, and SCB–33. Although As and Cr elements were less than the standard values, almost all samples were at the Threshold Effect Level (TEL). Based on the TEL quality standard for American PTEs by **Burton (2002)**, As had a value at the level of 5.9 mg/kg, while the Cr element was at 37.3 mg/kg. Apart from As and Cr elements, all PTEs also exceeded the quality standard values, as shown in **Table 2**.

The Fe was found to be below SQGs at SCB–06, SCB–09, SCB–10, SCB–12, SCB–13, and SCB–33. Apart from Fe, other PTEs, such as Ni at the SCB–05, SCB–06, and SCB–13 were less than SQGs. PTEs of Pb, Zn, Cd, and Cu had values less than the quality standard only at SCB–33. Meanwhile, the abundance of Mn exceeded the SQGs at all sampling points. The abundance of Mn elements could be attributed to various anthropo-

Copyright held(s) by author(s), publishing rights belongs to publisher, pp. 117-134, DOI: 10.17794/rgn.2023.4.10

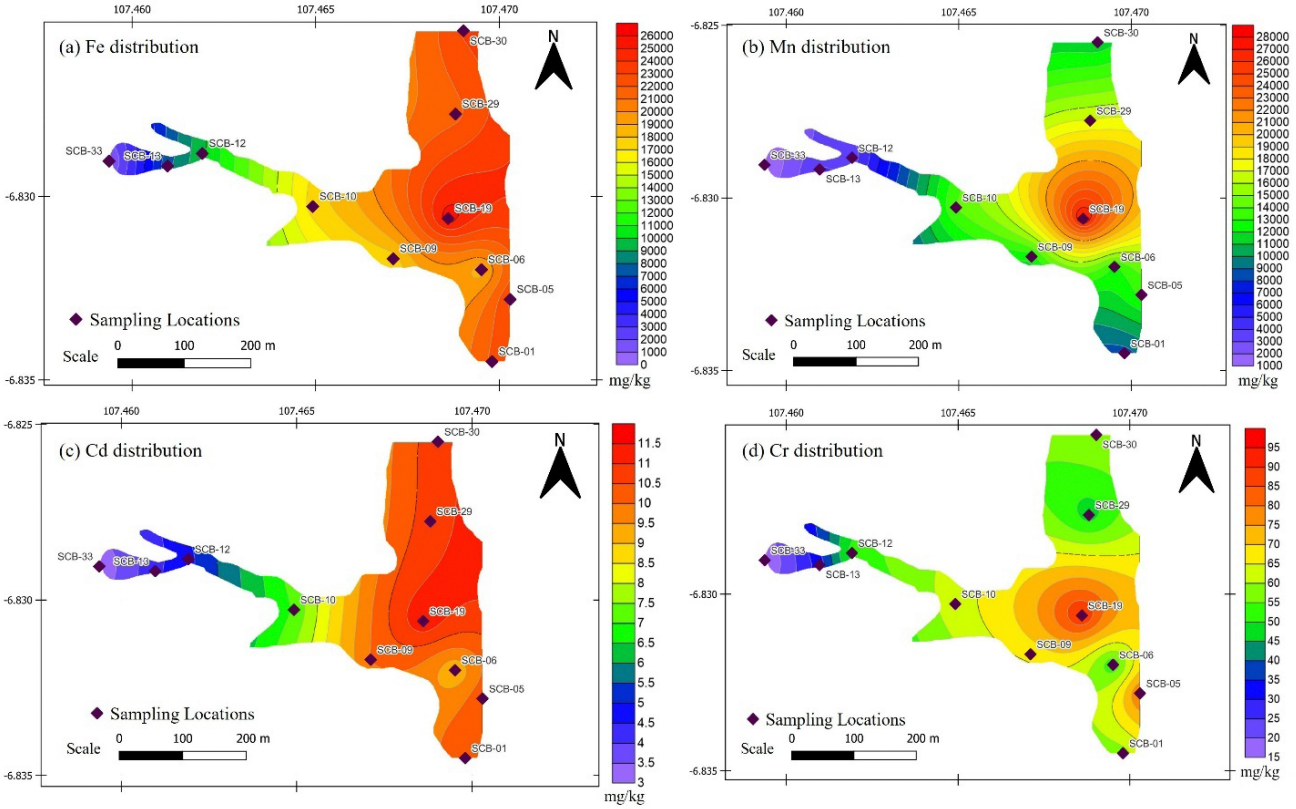

Figure 8: Map of distribution values of PTEs at sampling points (N: 11): (a) Fe; (b) Mn; (c) Cd; (d); Cr indicates that the highest values (the color scale towards red) is in the middle of the lake.

genic sources, such as industrial and mining activities, agriculture, as well as residential waste, electronic, industrial, and traffic waste (**Yunginger et al., 2018**). **Figure 8** shows the distribution map of several PTEs, such as Fe, Mn, Cd, and Cr. The highest content of Fe, Mn, Cd, and Cr was found at SCB–19, which was located in the middle of the lake. The high value of Fe, Mn, Cd, and Cr in the sediment could be caused by the emissions from vehicles and domestic waste (**Robertson et al., 2003**; **Chakarvorty et al., 2015**; **Yuan et al., 2019**).

Table 4 shows the results of pollution index calculation from PTEs content using I_{geo}, EF, CF, and PLI. The average results of the calculation of I_{geo}, EF, and CF sediment samples from Lake Ciburuy, from largest to smallest value was Cd > Mn > Cu > Pb > Zn > Co > As > Cr > Ni > Fe. The highest I_{geo} average value was shown by Cd and the level of contamination was categorized as highly to very highly polluted class. Since As, Cr, Ni, and Fe had a negative value, according to the table of I_{geo} contamination levels (**Muller, 1969**), the negative average I_{geo} value indicated that the surface sediments of Lake Ciburuy were not contaminated by As, Cr, Ni, and Fe. Similar results were also found in the sediments of the Hindon River, which reported that Fe, Zn, Ni, Mn, and Cr had negative values (**Chabukdhara and Nema, 2012**).

Based on the classification of EF values by **Hakanson (1980)**, the average value of EF calculation results for Lake Ciburuy sediment samples showed various enrichment levels. The Cd element was considered to have an extreme enrichment (EF = 59.49 mg/kg), while Mn had a very severe level (EF = 28.50 mg/kg). The average value of Cu, Pb, and Zn elements showed a severe level of enrichment (EF = 18.34; 14.74; 12.73). Meanwhile, other elements showed a minor level, such as the average value of EF in As, Cr, and Ni (EF = 2.01; 1.33; 1.02). The results showed that Co had a medium enrichment level (EF = 4.08), while Fe showed no EF (EF = 0.77), but at several sample points, it had a minor EF.

The results of the average CF calculation based on the classification level table by **Tomlinson (1980)** for Lake Ciburuy sediment samples found that the elements Cd, Mn, Cu, Pb, Zn, and Cu had a very high contamination level with the values of 27.99, 13.41, 8.63, 6.93, and 5.99, respectively. The Co element showed moderate contamination (CF = 1.92), while As, Cr, Ni, and Fe were at a low level (CF = 0.94, 0.62, 0.48, 0.36).

To evaluate the level of PTEs contamination related to anthropogenic activity, PLI was calculated. The calculation results at the sediment of Lake Ciburuy showed a range of 0.449 – 4.392. **Table 3** shows the results of PLI calculations for all sediment samples with a value of more than 1, except for the SCB–33.

The pollution index calculations by I_{geo}, EF, and CF showed that the sediments of Lake Ciburuy had average values of Mn, Pb, Zn, Cd, and Cu, which were classified as moderate to very severe contamination. This finding

Copyright held(s) by author(s), publishing rights belongs to publisher, pp. 117-134, DOI: 10.17794/rgn.2023.4.10

Table 3: Correlation table of physical and chemical properties using Pearson's formula. The results in bold show a significant correlation (*) at p < 0.05 and strong significant correlation (**) at p < 0.01.

Correlations																
	Fe	**Mn**	**Ni**	**Pb**	**Zn**	**As**	**Cd**	**Co**	**Cr**	**Cu**	**pH**	**EC**	**TDS**	χ_{LF}	χ_{FD}%	**PLI**
Fe	1															
Mn	**0.807****	1														
Ni	0.021	-0.192	1													
Pb	**0.878****	0.528	0.201	1												
Zn	0.421	0.185	**0.738****	**0.653***	1											
As	-0.363	-0.080	-0.241	-0.622*	-0.650*	1										
Cd	**0.964****	**0.778****	0.031	**0.887****	0.420	-0.275	1									
Co	**0.894****	0.586	-0.075	**0.831****	0.358	-0.422	**0.846****	1								
Cr	**0.834****	**0.783****	0.171	**0.642***	0.419	-0.183	**0.759****	**0.664***	1							
Cu	**0.864****	0.588	0.380	**0.944****	**0.718***	-0.447	**0.909****	**0.752****	**0.696***	1						
pH	-0.865**	-0.533	-0.312	-0.888**	-0.580	0.544	-0.816**	-0.712*	-0.675*	-0.855**	1					
EC	**0.637***	0.494	-0.055	**0.781****	0.527	-0.678*	**0.697***	**0.606***	0.361	**0.688***	-0.578	1				
TDS	0.642*	0.509	-0.073	**0.783****	0.510	-0.671*	**0.703***	**0.609***	0.359	**0.690***	-0.581	**0.999****	1			
χ_{LF}	0.483	0.306	-0.060	0.283	-0.004	-0.046	0.379	0.457	**0.675***	0.211	-0.367	0.093	0.069	1		
χ_{FD}	0.173	0.210	-0.060	0.377	0.258	-0.305	0.338	0.065	-0.197	0.388	-0.186	**0.653***	**0.667***	-0.558	1	
PLI	**0.916****	**0.785****	0.110	**0.794****	0.459	-0.246	**0.916****	**0.859****	**0.803****	**0.852****	-0.745**	0.593	**0.604***	0.340	0.140	1

was consistent with the abundance of PTEs, which revealed that these elements almost entirely exceeded the quality threshold. Furthermore, the Cd showed the highest I_{geo}, EF, and CF values at SCB–19. Several studies reported an abundance of this element around the lake derived from vehicle emissions and anthropogenic waste (**Chakarvorty et al., 2015**; **Yuan et al., 2019**). The results of EF calculations on the Cd element in lake waters had also been reported and it was considered to have a very extreme contamination factor. These results could be used as a reference for pollution in the lake due to particles entering the lake from streams (**Vrhovnik et al., 2013**).

5.3 Physical and Chemical Properties as Proxies of Pollution

The correlation between EC and TDS with PTEs is presented in **Table 3**. The EC and TDS values significantly correlated with the range r = 0.606 – 0.703 ($p<0.05$) for Fe, Cd, Co, and Cu. Meanwhile, these parameters had a significant correlation r = 0.781 – 0.783 ($p<0.01$) with Pb. The significant positive correlation between EC and TDS with PTEs indicated that the elements affected the parameters. The correlation between EC and Cd could be due to the insertion of external materials into the sediment, which had also been reported in other studies. The Cd content was found to increase with increasing ions in the sediment (**Miao et al., 2021**).

Apart from being correlated with PTEs, EC and TDS were also significantly correlated with χ_{FD}% (r = 0.653 – 0.667; $p<0.05$). The positive correlation between EC–TDS and χ_{FD}% indicated that the abundance of dissolved salts could contribute significantly to the formation of magnetic minerals. A similar result was also found in the Makoo region, Iran, which showed a considerable positive correlation, indicating the presence of ferrimagnetic minerals due to the high adsorption of dissolved salts in the soil affected by the increasing magnetic susceptibility values (**Ayoubi et al., 2019**).

The results also showed that there was a significant correlation between χ_{LF} and Cr (r = 0.675; $p <0.05$). These results could be interpreted that the more abundant the value χ_{LF}, the more Cr element content in the sample. The significant correlation between magnetic susceptibility and PTEs indicated that polluted samples contained high levels of PTEs with increasing magnetic susceptibility values (**Chan, 1999**). The high values in each element and magnetic susceptibility were probably due to the anthropogenic materials sources (**Spiteri et al., 2005**). Based on these findings, Lake Ciburuy sediment samples were polluted by anthropogenic materials sources.

Fe was found to have a very significant correlation r = 0.807 – 0.964 ($p< 0.01$) with almost all the elements, except for Ni, Zn, and As. Iron was generally the most abundant metal in all catchment areas because it was one

Copyright held(s) by author(s), publishing rights belongs to publisher, pp. 117-134, DOI: 10.17794/rgn.2023.4.10

Table 4: The calculation of pollution index. I_{geo}: Geo-accumulation Index, EF: Enrichment Factor, CF: Contaminant Factor, PLI: Pollution Load Index. SD: Standard Deviation.

Sample ID	I_{geo} (mg/kg)										
	Fe	Mn	Ni	Pb	Zn	As	Cd	Co	Cr	Cu	
SCB–01	-1.67	2.75	-0.85	2.60	2.28	-0.57	4.53	0.73	-1.22	3.05	
SCB–05	-1.61	3.39	-2.67	2.47	1.91	-0.73	4.54	0.84	-0.72	2.67	
SCB–06	-1.94	3.33	-6.69	2.57	2.01	-1.33	4.33	0.09	-1.43	2.68	
SCB–09	-2.02	3.28	-0.60	2.58	3.05	-0.79	4.48	0.04	-1.02	3.18	
SCB–10	-2.02	3.46	-1.43	2.13	2.68	-2.27	3.97	0.52	-1.11	2.44	
SCB–12	-2.86	1.42	-1.74	1.85	1.80	-1.28	3.43	-0.39	-1.37	1.94	
SCB–13	-3.20	1.70	-2.46	0.93	1.49	-0.23	3.29	-1.14	-2.05	1.06	
SCB–19	-1.47	4.43	-	2.17	1.13	0.19	4.67	0.66	-0.56	2.73	
SCB–29	-1.71	3.74	-	2.53	1.79	-1.76	4.58	0.73	-1.52	2.74	
SCB–30	-1.61	3.15	-	2.78	2.20	-1.06	4.59	1.29	-1.16	2.94	
SCB–33	-6.44	-0.34	-	-1.93	-4.12	0.36	2.79	-2.50	-3.18	-0.30	
MAX	-1.47	4.43	-0.60	2.78	3.05	0.36	4.67	1.29	-0.56	3.18	
MIN	-6.44	-0.34	-6.69	-1.93	-4.12	-2.27	2.79	-2.50	-3.18	-0.30	
MEAN	-2.41	2.75	-2.35	1.88	1.47	-0.86	4.11	0.08	-1.39	2.28	
SD	1.44	1.34	2.06	1.37	1.93	0.80	0.65	1.09	0.72	1.04	
	EF (mg/kg)										
	Fe	Mn	Ni	Pb	Zn	As	Cd	Co	Cr	Cu	
SCB–01	1.00	21.38	1.77	19.35	15.43	2.15	73.59	5.30	1.37	26.39	
SCB–05	1.05	33.32	0.50	17.70	11.99	1.92	74.10	5.69	1.94	20.28	
SCB–06	0.83	31.97	0.03	18.95	12.87	1.26	64.05	3.39	1.19	20.48	
SCB–09	0.79	30.88	2.10	19.06	26.45	1.85	71.08	3.28	1.57	28.85	
SCB–10	0.78	35.10	1.19	14.00	20.38	0.66	49.98	4.58	1.48	17.34	
SCB–12	0.44	8.55	0.96	11.50	11.12	1.32	34.44	2.44	1.23	12.26	
SCB–13	0.35	10.35	0.58	6.08	8.95	2.71	31.10	1.45	0.77	6.66	
SCB–19	1.15	68.56	-	14.36	6.98	3.64	80.91	5.03	2.17	21.13	
SCB–29	0.98	42.63	-	18.37	11.00	0.94	76.11	5.28	1.11	21.34	
SCB–30	1.04	28.26	-	21.90	14.65	1.53	76.97	7.82	1.42	24.43	
SCB–33	0.04	2.52	-	0.84	0.18	4.09	22.09	0.56	0.35	2.58	
MAX	1.15	68.56	2.10	21.90	26.45	4.09	80.91	7.82	2.17	28.85	
MIN	0.04	2.52	0.03	0.84	0.18	0.66	22.09	0.56	0.35	2.58	
MEAN	0.77	28.50	1.02	14.74	12.73	2.01	59.49	4.08	1.33	18.34	
SD	0.35	18.28	0.73	6.41	6.85	1.09	21.29	2.09	0.50	8.12	
	CF (mg/kg)										PLI
	Fe	Mn	Ni	Pb	Zn	As	Cd	Co	Cr	Cu	
SCB–01	0.47	10.06	0.83	9.10	7.26	1.01	34.62	2.49	0.64	12.42	3.36
SCB–05	0.49	15.68	0.24	8.33	5.64	0.91	34.86	2.68	0.91	9.54	3.02
SCB–06	0.39	15.04	0.01	8.92	6.06	0.59	30.13	1.59	0.56	9.63	1.93
SCB–09	0.37	14.53	0.99	8.97	12.44	0.87	33.44	1.55	0.74	13.57	3.49
SCB–10	0.37	16.51	0.56	6.59	9.59	0.31	23.51	2.16	0.70	8.16	2.68
SCB–12	0.21	4.02	0.45	5.41	5.23	0.62	16.20	1.15	0.58	5.77	1.82
SCB–13	0.16	4.87	0.27	2.86	4.21	1.27	14.63	0.68	0.36	3.13	1.44
SCB–19	0.54	32.25	-	6.76	3.28	1.71	38.07	2.37	1.02	9.94	4.39
SCB–29	0.46	20.06	-	8.64	5.17	0.44	35.81	2.49	0.52	10.04	3.53
SCB–30	0.49	13.29	-	10.30	6.89	0.72	36.21	3.68	0.67	11.49	4.12
SCB–33	0.02	1.19	-	0.39	0.09	1.93	10.39	0.26	0.17	1.22	0.45
MAX	0.54	32.25	0.99	10.30	12.44	1.93	38.07	3.68	1.02	13.57	0.45
MIN	0.02	1.19	0.01	0.39	0.09	0.31	10.39	0.26	0.17	1.22	4.39
MEAN	0.36	13.41	0.48	6.93	5.99	0.94	27.99	1.92	0.62	8.63	2.75
SD	0.16	8.60	0.34	3.01	3.22	0.51	10.01	0.98	0.24	3.82	1.21

Copyright held(s) by author(s), publishing rights belongs to publisher, pp. 117-134, DOI: 10.17794/rgn.2023.4.10

Table 5: Clusters of samples (N = 11) based on physical-chemical properties and magnetic parameters features obtained from a non-hierarchical k-means cluster analysis. SD: Standard Deviation.

Variable	Mean Overall	SD	Cluster 1 (n=3)		Cluster 2 (n=6)		Cluster 3 (n=2)	
			Mean group	SD	Mean group	SD	Mean group	SD
pH	7.64	0.48	8.20	0.61	7.42	0.23	7.45	0.07
EC (µS/cm)	370.00	210.86	140.00	101.49	488.33	181.59	360.00	127.28
TDS (mg/L)	270.91	149.97	107.67	74.44	355.67	130.91	261.50	70.00
c_{LF} ($\times 10^{-8}$ m^3/kg)	1003.73	904.29	625.21	574.67	698.62	261.89	2486.82	1336.62
c_{FD}%	3.27	1.82	2.08	1.07	4.38	1.67	1.73	0.61
Fe (mg/kg)	17050.50	7766.35	6090.78	4675.73	20069.59	2553.06	24432.83	1677.38
Mn (mg/kg)	11397.64	7310.26	2855.53	1640.13	12677.81	2828.99	20370.28	9962.46
Ni (mg/kg)	32.57	24.45	16.40	15.43	27.13	30.82	8.03	11.35
Pb (mg/kg)	138.68	60.28	57.77	50.20	175.08	24.16	150.85	22.26
Zn (mg/kg)	568.85	305.95	301.81	258.86	750.69	254.02	423.91	158.25
As (mg/kg)	12.27	6.64	16.56	8.49	8.55	3.40	17.02	7.43
Cd (mg/kg)	8.40	3.00	4.12	0.90	9.69	1.45	10.94	0.68
Co (mg/kg)	36.43	18.70	13.27	8.40	44.18	14.86	47.93	4.18
Cr (mg/kg)	56.19	21.22	33.22	18.73	57.44	7.44	86.89	6.99
Cu (mg/kg)	388.26	172.00	151.75	102.90	489.82	89.23	438.35	12.65
PLI	2.75	1.21	1.24	0.71	3.18	0.77	3.71	0.97

of the most common elements in the Earth's crust (**Usero et al., 2004**). Furthermore, the highest correlation between Fe and PTEs was with Cd ($r = 0.964$; $p < 0.01$). This strong correlation, which was found in the lake sediment had been reported in agriculture and industry areas (**Goher et al., 2014**; **Redwan et al., 2022**). The results showed that there was also a significant correlation between Fe and Pb ($r = 0.878$; $p<0.01$). The high correlations indicate that these parameters are built by the same mechanism and common source (**Abderrahmane et al., 2021**). This indicated that there were emissions derived from vehicles (**Robertson et al., 2003**). However, the presence of a lot of Fe could also indicate that the sample contained anthropogenic material, one of which came from motor vehicle emissions (**Zhang et al., 2012**). This was important because Lake Ciburuy was close to urban roads, residential areas, and a tourist area. There were also rice fields, agriculture, and industrial areas around the lake, which produced anthropogenic materials.

Apart from Fe, Cd had a high correlation with almost elements, except Ni, Zn, and As. Based on these results, the content of the Cd element in the sediments of Lake Ciburuy could be used to determine the source of pollutants. This finding was strengthened by the results of I_{geo}, EF, and CF values, where it was considered to have very extreme contamination levels. PLI calculations at all sampling points showed that the sediment was contaminated by anthropogenic material, except SCB–33. **Table 3** also shows a strong significant correlation between PLI and PTEs except for Ni, Zn, and As. Furthermore, PLI also had a significant correlation with the physical properties of TDS ($r = 0.604$, $p<0.05$). The difference in the correlation between the magnetic parameters and the PTEs was due to the involvement of magnetic mineral concentrations, which were influenced by the mineral phase, grain size or presence of different source mixtures. The mineral concentration was also affected by the physical and chemical changes that occurred during transportation and deposition (**Yang et al., 2010**). This analysis showed that the significant correlation between PLI and PTEs as well as physical properties could be used as a proxy for pollution.

The result of the PCA analysis of physical-chemical properties is presented in **Figure 9**. The closer the variable position was to the principal component, the higher the value of positive correlation. Meanwhile, the difference in position and coordinate (quadrant) described the direction of positive and negative correlation. **Figure 9** shows that there were loading results and scores from the principal component (PC1 and PC2). PC1 (57.9% of the total variance) had strong positive loadings on EC, TDS, Fe, Mn, Pb, Cr, Cd, Co, Cu, and PLI as well as negative loadings on pH and As. The results also showed that PC2 with 16% of the total variance had positive loadings on χ_{LF}. The first quadrant revealed that SCB–05 and SCB–19 were highly influenced by parameters χ_{LF} and could be affected by several PTEs, such as Cr, Mn, Fe, Cd, Co, and PLI. SCB–01, SCB–06, SCB–09, SCB–10, SCB–29, and SCB–30 in the fourth quadrant were influenced by Cd, Cu, Pb, EC, TDS, Zn, χ_{FD}%, and Ni.

Table 5 provides information on all the variables used for cluster analysis (CA). CA connected cluster groups based on the homogeneity of the variables studied, as shown in **Figure 9**. Based on several variables, cluster 3 consisted of the parameter with the highest value of χ_{LF}

Copyright held(s) by author(s), publishing rights belongs to publisher, pp. 117-134, DOI: 10.17794/rgn.2023.4.10

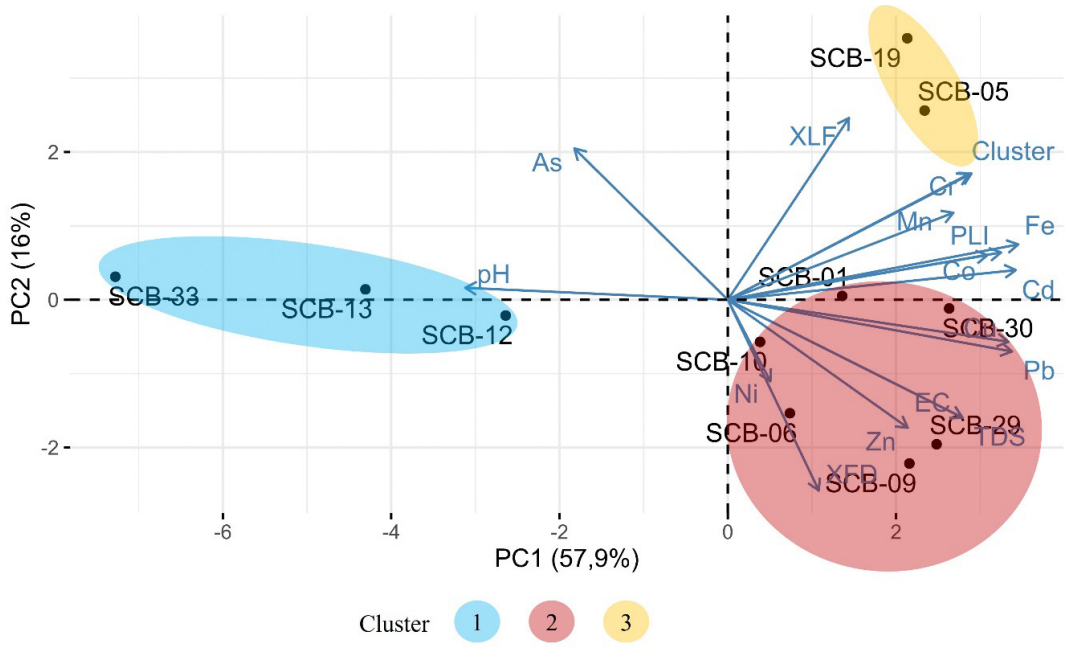

Figure 9: Multivariate analysis by Principal Component Analysis (PCA) and clustering sediment samples (N = 11). PCA's result is indicated by the blue arrow. Cluster analysis (CA) based on the variables physical-chemical properties and magnetic parameter. The sites were classified into three groups, showing group 1 is low contamination (blue), group 2 is medium contamination (red) and group 3 is high contamination (yellow).

at SCB–05 on the edge of the lake close to residential areas. It also contained several elements of Fe, Mn, Cd, and Cr, with the highest values at SCB–19 in the middle of the lake. Furthermore, the medium cluster indicated by cluster 2 contained samples SCB–01, SCB–06, SCB–09, SCB–10, SCB–29, and SCB–30, which were located in the water bodies. Cluster 1 showed a low value of physical-chemical properties of samples SCB–12, SCB–13, and SCB–33 compared to other sampling points. These sampling points were near rice fields, irrigation, and marble waste, respectively.

6. Conclusions

Based on the results and discussion on the physical and chemical properties of sediments, several conclusions could be written as follows:

1. Measurement of physical properties EC, TDS, and pH indicated that anthropogenic material was present in Lake Ciburuy sediments. This indication was strengthened by the magnetic parameter results, which showed a high magnetic susceptibility value of χ_{LF} with an average value of 1010.905 × 10^{-8} m^3/kg. The average value of χ_{FD}% was 3.731%, indicating that the sediment of Lake Ciburuy contained anthropogenic material. Furthermore, these findings were strengthened by the results of the scattergram plot of χ_{LF} and χ_{FD}%. This plot showed that the sediments were dominated by mixed grains of SSD or MD, denoting the presence of anthropogenic material. This analysis was consistent with the results of Day's plot that the sediment grains of Lake Ciburuy had a mixture of MD. The results of XRD measurements, hysteresis curves, and SEM–EDS also confirmed that the area was dominated by magnetite minerals, with spherule-shaped grains.
2. The measurement of the chemical properties showed that the element content of Mn, Pb, Zn, Cd, and Cu could be a source of pollutants because they had an abundance of PTEs exceeding the sediment quality standards, with a very high level of pollution. This result was strengthened by the calculated pollution index, where sample points showed a value >1 except SCB–33, indicating the presence of pollution.
3. The significant correlation between physical-chemical properties and magnetic parameters, such as EC and TDS with χ_{FD}%, χ_{LF}, and Cr; Fe and Cd; Fe and Pb; PLI and PTEs (Fe, Mn, Pb, Cd, Co, Cr, Cu), as well as PLI and TDS, indicated the potential of physical-chemical properties as a proxy indicator of pollution due to anthropogenic material.

Acknowledgement

The authors are grateful to Universitas Padjadjaran for financial support through Unpad Internal Research Grants 2022 with a scheme of RKDU (Contract number: 2203/UN6.3.1/PT.00/2022). The authors are also grate-

ful to Azmi Sauqi for the assistance provided during statistical analysis.

7. References

Abderrahmane, B., Naima, B., Tarek, M., and Abdelghani, M. (2021): Influence of highway traffic on contamination of roadside soil with heavy metals. Civil Engineering Journal, 7(8), 1459-1471.

Adekola, F.A. and Eletta, O.A.A. (2007): A study of heavy metal pollution of Asa River, Ilorin. Nigeria; trace metal monitoring and geochemistry. Environmental Monitoring and Assessment, 125(1), 157-163.

Ayoubi, S., Abazari, P. and Zeraatpisheh, M. (2018): Soil great groups discrimination using magnetic susceptibility technique in a semi-arid region, central Iran. Arabian Journal of Geosciences, 11(20), 1-12.

Ayoubi, S., Adman, V. and Yousefifard, M. (2019): Use of magnetic susceptibility to assess metals concentration in soils developed on a range of parent materials. Ecotoxicology and environmental safety, 168, 138-145.

Barbieri, M.J.J.G.G. (2016): The importance of enrichment factor (EF) and geoaccumulation index (Igeo) to evaluate the soil contamination. J Geol Geophys, 5(1), 1-4.

Bijaksana, S. and Huliselan, E.K. (2010): Magnetic properties and heavy metal content of sanitary leachate sludge in two landfill sites near Bandung, Indonesia. Environmental Earth Sciences, 60(2), 409-419.

Burton Jr, G.A. (2002): Sediment quality criteria in use around the world. Limnology, 3(2), 65-76.

Chabukdhara, M. and Nema, A.K. (2012): Assessment of heavy metal contamination in Hindon River sediments: a chemometric and geochemical approach. Chemosphere, 87(8), 945-953.

Chakarvorty, M., Dwivedi, A.K., Shukla, A.D., Kumar, S., Niyogi, A., Usmani, M. and Pati, J. K. (2015): Geochemistry and magnetic measurements of suspended sediment in urban sewage water vis-à-vis quantification of heavy metal pollution in Ganga and Yamuna Rivers, India. Environmental Monitoring and Assessment, 187(9), 1-17.

Chan, L.S., Yeung, C.H., Yim, W.S. and Or, O.L. (1998): Correlation between magnetic susceptibility and distribution of heavy metals in contaminated sea-floor sediments of Hong Kong Harbour. Environmental Geology, 36, 77-86.

Chaparro, M.A.E., Chaparro, M.A.E., Córdoba, F.E., Lecomte, K.L., Gargiulo, J.D., Barrios, A.M., Uran, G.M., Czalbowski, N.T.M., Lavat, A. and Böhnel, H.N. (2017): Sedimentary analysis and magnetic properties of Lake Anónima, Vega Island. Antarctic Science, 29(5), 429-444.

Cook, H.E., Johnson, P.D., Matti, J.C. and Zemmels, I. (1975): IV. Methods of sample preparation, and X-ray diffraction data analysis, X-ray mineralogy laboratory, Deep Sea Drilling Project, University of California, Riverside. Initial reports of the deep sea drilling project, 25, 999-1007.

Dankoub, Z., Ayoubi, S., Khademi, H. and Sheng-Gao, L.U. (2012): Spatial distribution of magnetic properties and selected heavy metals in calcareous soils as affected by land use in the Isfahan region, Central Iran. Pedosphere, 22(1), 33-47.

Dearing, J. (1999): Environmental magnetic susceptibility using the Bartington MS2 system. Bartington Instruments Ltd. British Library London.

Désirée, N.T.S., Zacharie, E.B.A., Brice, T.K., Ange, W.K.S., Jacques, E. and Paul, B. (2021): Heavy metal contamination and ecological risk assessment of overlying water and sediments of Nkozoa Lake (Southern Cameroon). Annual Research & Review in Biology, 92-109.

El-Sayed, H.A., Farag, A.B., Kandeel, A.M., Younes, A.A. and Yousef, M.M. (2018): Characteristics of the marble processing powder waste at Shaq El-Thoaban industrial area, Egypt, and its suitability for cement manufacture. HBRC journal, 14(2), 171-179.

Evans, M.E. and Heller, F. (2003): Environmental magnetism: principles and applications of enviromagnetics. Elsevier.

Fitriani, D., Utami, W., Kirana, K.H., Agustine, E. and Zulaikah, S. (2021): Magnetic Signatures on River Sediments and Agricultural Soils as Proxy Indicators of Anthropogenic-derived Pollution Case Study: Cikijing River, Rancaekek, West Java. Jurnal Penelitian Pendidikan IPA, 7(3), 381-387.

Franke, C., von Dobeneck, T., Drury, M.R., Meeldijk, J.D. and Dekkers, M.J. (2007): Magnetic petrology of equatorial Atlantic sediments: Electron microscopy results and their implications for environmental magnetic interpretation. Paleoceanography, 22(4).

Gehring, A.U., Fischer, H., Louvel, M., Kunze, K. and Weidler, P.G. (2009): High temperature stability of natural maghemite: a magnetic and spectroscopic study. Geophysical Journal International, 179(3), 1361-1371.

Goher, M.E., Farhat, H.I., Abdo, M.H. and Salem, S.G. (2014): Metal pollution assessment in the surface sediment of Lake Nasser, Egypt. The Egyptian Journal of Aquatic Research, 40(3), 213-224.

Hakanson, L. (1980). An ecological risk index for aquatic pollution control. A sedimentological approach. Water research, 14(8), 975-1001.

Hamdan, A.M., Kirana, K.H., Hakim, F., Iksan, M., Bijaksana, S., Mariyanto, M., Ashari, T.M., Ngkoimani, L.O., Kurniawan, H., Pratama, A. and Wahid, M.A. (2022): Magnetic susceptibilities of surface sediments from estuary rivers in volcanic regions. Environmental Monitoring and Assessment, 194(4), 239.

Herbatani, (2021): 5 Cara Membuat Pelet Ikan dengan Mudah, Pusat Informasi Tanaman Obat, Kesehatan dan Pertanian. Available at: https://herbatani.com/5-cara-membuat-pelet-ikan-dengan-mudah/ (Accessed: 24 June 2022).

Iswanto, B. H., Pratiwi, I., & Zulaikah, S. (2020). Identification of environments based on magnetic susceptibility and geochemical data using multivariate statistical analysis. In AIP Conference Proceedings (Vol. 2251, No. 1, p. 040005). AIP Publishing LLC.

Kirana, K.H., Apriliawardani, J., Ariza, D., Fitriani, D., Agustine, E., Bijaksana, S., Fajar, S.J. and Nugraha, M.G. (2021): Frequency Dependent Magnetic Susceptibility in Topsoil of Bandung City, Indonesia. In IOP Conference Series: Earth and Environmental Science (Vol. 873, No. 1, p. 012016). IOP Publishing.

Copyright held(s) by author(s), publishing rights belongs to publisher, pp. 117-134, DOI: 10.17794/rgn.2023.4.10

Lu, S.G., Bai, S.Q. and Xue, Q.F. (2007): Magnetic properties as indicators of heavy metals pollution in urban topsoils: a case study from the city of Luoyang, China. Geophysical Journal International, 171(2), 568-580.

Madhulekha, S.A. and Agarwal, S. (2017): Study of Correlation Coefficient for Physico-chemical parameter to assess the water quality of river Ganga at Kanpur, India. International Journal of Innovative Research in Science, Engineering and Technology, 6(8), 1-6.

Mariyanto, M., Amir, M.F., Utama, W., Bijaksana, S., Pratama, A., Yunginger, R. and Sudarningsih, S. (2019): Heavy metal contents and magnetic properties of surface sediments in volcanic and tropical environment from Brantas River, Jawa Timur Province, Indonesia. Science of The Total Environment, 675, 632-641.

Miao, X., Hao, Y., Liu, H., Xie, Z., Miao, D. and He, X. (2021): Effects of heavy metals speciations in sediments on their bioaccumulation in wild fish in rivers in Liuzhou—A typical karst catchment in southwest China. Ecotoxicology and Environmental Safety, 214, 112099.

Miler, M. and Gosar, M. (2015): Chemical and morphological characteristics of solid metal-bearing phases deposited in snow and stream sediment as indicators of their origin. Environmental Science and Pollution Research, 22, 1906-1918.

Moskowitz, B. M. (1991). Hitchhiker's guide to magnetism. In Environmental Magnetism Workshop (IRM) (Vol. 279, No. 1, p. 48). Univ. of Minn., Minneapolis, Minn: Inst. for Rock Magnetism.

Muller, G. (1969): Index of geoaccumulation in sediments of the Rhine River. Geojournal, 2, 108-118.

Nurqolbi, Y.P. and Hindersah, H. (2019): Kajian Pelestarian Kawasan Pariwisata Situ Ciburuy. Prosiding Perencanaan Wilayah Dan Kota, 0(0), 91–99

Pandey. M., Pandey. A.K. Mishra. A. and Tripathi. B.D. (2015): Assessment of metal species in river Ganga sediment at Varanasi. India using sequential extraction procedure and SEM–EDS. Chemosphere. 134. 466-474.

Ramasamy, V., Senthil, S., Paramasivam, K. and Suresh, G. (2022): Potential toxicity of heavy metals in beach and intertidal sediments: A comparative study. Acta Ecologica Sinica, 42(2), 57-67.

Redwan, M. and Elhaddad, E. (2022): Heavy metal pollution in Manzala Lake sediments, Egypt: sources, variability, and assessment. Environmental Monitoring and Assessment, 194(6), 1-16.

Robertson, D.J., Taylor, K.G. and Hoon, S.R. (2003): Geochemical and mineral magnetic characterisation of urban sediment particulates, Manchester, UK. Applied geochemistry, 18(2), 269-282.

Rusydi, A.F. (2018): Correlation between conductivity and total dissolved solid in various type of water: A review. In IOP conference series: earth and environmental science (Vol. 118, No. 1, p. 012019). IOP Publishing.

Schmidt, A., Yarnold, R., Hill, M. and Ashmore, M. (2005): Magnetic susceptibility as proxy for heavy metal pollution: a site study, J. Geochem. Explor., 85, 109–117.

Skorbiłowicz, E., Rogowska, W., Skorbiłowicz, M. and Ofman, P. (2022): Spatial Variability of Metals in Coastal Sediments of Ełckie Lake (Poland). Minerals, 12(2), 173.

Solomon, J.S., Ahmed, A.L., Adamu, I.H. and Dimu, O.O. (2017): Identifying anthropogenic metallic pollutants using frequency dependent magnetic susceptibility measurements in Abuja Metropolis. Currents Trends In Natural Sciences, 6(11), 13-22.

Spiteri, C., Kalinski, V., Rösler, W., Hoffmann, V., Appel, E. and Magprox Team. (2005): Magnetic screening of a pollution hotspot in the Lausitz area, Eastern Germany: correlation analysis between magnetic proxies and heavy metal contamination in soils. Environmental Geology, 49, 1-9.

Su, Y., Gao, X., Liu, Q., Hu, P., Duan, Z., Jiang, Z., Wang, J., Zhu, L., Doberschütz, S., Mäusbacher, R. and Daut, G. (2013): Mechanism of variations in environmental magnetic proxies of lake sediments from Nam Co, Tibet during the Holocene. Chinese Science Bulletin, 58(13), 1568-1578.

Sudarningsih, S., Bijaksana, S., Ramdani, R., Hafidz, A., Pratama, A., Widodo, W., Iskandar, I., Dahrin, D., Jannatul Fajar, S. and Agus Santoso, N. (2017): Variations in the concentration of magnetic minerals and heavy metals in suspended sediments from Citarum river and its tributaries, West Java, Indonesia. Geosciences, 7(3), 66.

Sudjatmiko. (1972): Peta Geologi Regional lembar Cianjur, Jawa. Pusat Penelitian Dan Pengembangan Geologi, 1.

Supriyatna, A., Ramdani, R.R. and Suhendar, D.S. (2013): Korelasi Kandungan Besi Terlarut Terhadap Kelimpahan Phytoconis Sp. Pada Perairan Situ Ciburuy Kabupaten Bandung Barat. JURNAL ISTEK, 7(1).

Tamuntuan, G., Bijaksana, S., Gaffar, E., Russell, J., Safiuddin, L.O. and Huliselan, E. (2010): The magnetic properties of Indonesian Lake Sediment: A case study of a tectonic lake in South Sulawesi and maar lakes in East Java. ITB Journal of Science A, 42, 31-48.

Tamuntuan, G., Bijaksana, S., King, J., Russell, J., Fauzi, U., Maryunani, K. and Aufa, N. (2015): Variation of magnetic properties in sediments from Lake Towuti, Indonesia, and its paleoclimatic significance. Palaeogeography, Palaeoclimatology, Palaeoecology, 420, 163-172.

Tomlinson, D.L., Wilson, J.G., Harris, C.R., & Jeffrey, D.W. (1980): Problems in the assessment of heavy-metal levels in estuaries and the formation of a pollution index. Helgoländer meeresuntersuchungen, 33(1), 566-575.

Usero, J., Izquierdo, C., Morillo, J. and Gracia, I. (2004): Heavy metals in fish (Solea vulgaris, Anguilla anguilla and Liza aurata) from salt marshes on the southern Atlantic coast of Spain. Environment international, 29(7), 949-956.

Vrhovnik, P., Šmuc, N.R., Dolenec, T., Serafimovski, T. and Dolenec, M. (2013): An evaluation of trace metal distribution and environmental risk in sediments from the Lake Kalimanci (FYR Macedonia). Environmental Earth Sciences, 70(2), 761-775.

Wedepohl, K.H. (1971): Environmental influences on the chemical composition of shales and clays. Physics and Chemistry of the Earth, 8, 307-333.

Yang, T., Liu, Q., Li, H., Zeng, Q. and Chan, L. (2010): Anthropogenic magnetic particles and heavy metals in the

Copyright held(s) by author(s), publishing rights belongs to publisher, pp. 117-134, DOI: 10.17794/rgn.2023.4.10

road dust: Magnetic identification and its implications. Atmospheric Environment, 44(9), pp.1175-1185.

Yang, T., Liu, Q., Zeng, Q. and Chan, L. (2009): Environmental magnetic responses of urbanization processes: evidence from lake sediments in East Lake, Wuhan, China. Geophysical Journal International, 179(2), 873-886.

Yuan, Z., Luo, T., Liu, X., Hua, H., Zhuang, Y., Zhang, X., Zhang, L., Zhang, Y, Xu, W. and Ren, J. (2019): Tracing anthropogenic cadmium emissions: from sources to pollution. Science of the total environment, 676, 87-96.

Yunginger, R., Bijaksana, S., Dahrin, D., Zulaikah, S., Hafidz, A., Kirana, K.H., Sudarningsih, S., Mariyanto, M. and Fajar, S.J. (2018): Lithogenic and anthropogenic components in surface sediments from lake limboto as shown by magnetic mineral characteristics, trace metals, and REE geochemistry. Geosciences, 8(4), 116.

Zhang, C., Qiao, Q., Appel, E. and Huang, B. (2012): Discriminating sources of anthropogenic heavy metals in urban street dusts using magnetic and chemical methods. Journal of Geochemical Exploration, 119, 60-75.

SAŽETAK

Identifikacija antropogenih materijala u sedimentima jezera Ciburuy korištenjem fizičko-kemijskih svojstava i indeksa onečišćenja

Područje jezera Ciburuy pod velikim je utjecajem širokoga spektra ljudskih aktivnosti, uključujući stambena područja, rižina polja, stočarstvo, plantaže, gust promet vozila i razne industrije, što dovodi do nakupljanja zagađivača. Čestice nastale antropogenim aktivnostima odnijet će se i taložiti s erodiranim tlom i postati sediment u jezeru. To bi moglo stvoriti ozbiljne probleme u vodenome okolišu ako ne postoji studija praćenja. Stoga je cilj ove studije bio identificirati antropogeni materijal proizveden ljudskim aktivnostima korištenjem analize fizičkih i kemijskih svojstava i izračuna indeksa onečišćenja. Analiza fizičkih svojstava pokazala je da su električna vodljivost (EC), ukupna otopljena krutina (TDS) i magnetska osjetljivost po redu unutar raspona 30 – 790 μS/cm, 29 – 555 mg/L, 7,310 – 3431,956 $\times 10^{-8}$ m^3/kg. Difrakcija rendgenskih zraka (XRD) i parametar histereze pokazali su da uzorci sadržavaju ferimagnetske materijale, posebno magnetit s pseudojednodomenskom (PSD) i višedomenskom (MD) mješavinom. Skenirajući elektronski mikroskop (SEM) i energetska disperzivna spektroskopija (EDS) identificirali su morfologiju magnetskoga minerala s različitim oblicima, kao što su oktaedar i sferula. Nadalje, oblik sferule upućuje na prisutnost antropogenih materijala u uzorku. Što se tiče kemijskih svojstava, ova studija mjeri pH i potencijalno toksične elemente (PTE) u sedimentima. pH je bio u rasponu 7,2 – 8,9, dok su PTE pokazivali umjerenu do vrlo jaku razinu kontaminacije Mn, Pb, Zn, Cd i Cu, što je premašilo standard kvalitete sedimenta. PCA otkriva međusobnu vezu između fizičkih i kemijskih svojstava, koja mogu identificirati zagađivače koji potječu od antropogenih materijala, kao i uputiti na niske, srednje i visoke razine onečišćenja u području jezera.

Ključne riječi:
antropogenost, fizička i kemijska svojstva, indeks onečišćenja

Authors' contribution

Mileani Shafaria (1) (S.Sci., M.Sci. student) performed the fieldwork, conducted measurements and processing on magnetic and geochemistry data collections, performed data interpretation, prepared the original and final manuscript. **Kartika Hajar Kirana (2)** (Ph.D., Associate Professor in Geophysics) provided magnetic data interpretation and statistical analysis, prepared the original and final manuscript. **Dini Fitriani (3)** (Ph.D., Associate Professor in Geophysics) provided geochemical data interpretation, prepared the original and final manuscript. **Eleonora Agustine (4)** (Ph.D., Assistant Professor in Geophysics) provided electrical conductivity, total dissolved solid, and pH data interpretation, prepared the original and final manuscript. **Asep Harja (5)** (Ph.D., Associate Professor in Geophysics) provided litology interpretation of the study area, prepared the original and final manuscript. **Cipta Endyana (5)** (Ph.D., Associate Professor in Geological Engineering) provided geology interpretation of the study area, prepared the original and final manuscript.

Copyright held(s) by author(s), publishing rights belongs to publisher, pp. 117-134, DOI: 10.17794/rgn.2023.4.10